

# Nanoporous LaAlO<sub>3</sub> system: Synthesis and evaluation of versatile properties along with their gas sensing potential

Mrs. Gore G. S<sup>1</sup>, Mrs. Kailas Gandhi<sup>1</sup>, Dr. G. B. Sathe<sup>1</sup>, Dr. B. A. Yamgar<sup>1</sup>, S. S. Marathe<sup>1</sup>,  
A. V. Dinde<sup>1</sup>, D. D. Kulkarni<sup>1</sup>, M. N. Lad<sup>1</sup>, Dr. Kashmiri A. Khamkar<sup>2</sup>, Dr. Viashali B. Adsul<sup>3</sup>

E-mail ggore3@gmail.com

<sup>1</sup>Department of Chemistry, D. U. B. Senior Science College, Dapoli, Dist.: Ratnagiri 415712 (MS), India.

<sup>2</sup>Department of Chemistry, MIT College Pune 411038

<sup>3</sup>Department of Chemistry, Bharati Vidyapeeth University, Yashwantrao Mohite College, Pune 411038 (MS), India.

## INTRODUCTION:

Measurement and control of humidity is imperative in many areas including meteorology, medicine, food production, agriculture and domestic environment. The measurement of relative humidity seems to be very convenient for the humidity detection [1-5]. Metal oxides have been widely investigated for the above purpose at both elevated and room temperatures as the surface and open pores tend to collect the water vapor by adsorption and condensation. Therefore the electrical properties are largely related to their porosity [6-10]. Auto-combustion technique finds to be a promising method as it is applicable for high purity mixed metal oxides with homogeneous distribution of components on the atomic scale.

The research in nano-science may be aimed to explore synthesis and understand new nanomaterials as well as the related phenomena [11-17]. We discuss here the synthesis of LaAlO<sub>3</sub> nanoparticles by sol-gel auto-combustion method which is a unique combination of the ignition and chemical gelation processes. This method has the advantages of simple preparation, cost-effective and gentle chemistry route resulting in ultra-fine and homogeneous powder.

## EXPERIMENTAL DETAILS:

The LaAlO<sub>3</sub> is prepared by the sol-gel auto-combustion method. The reagents used are lanthanum nitrate, aluminum nitrate and glycine. An appropriate amount of metal nitrates and glycine are first dissolved in a minimum amount of water. The molar ratio of nitrates is 1:1 and nitrates to glycine are 1:2. The final solution is evaporated on hot plate at temperature range 80-90°C until a thick gel is formed. The gel was kept on a hot plate for auto-combustion and heated in the temperature range of 160-180°C. The nanocrystalline LaAlO<sub>3</sub> powder was formed within five minutes. This was further annealed in the air at 800°C for 4 hours. The sintered material was mixed with 2% PVA as binder and pressed in to pellets with subsequent heating at 500°C to remove the excess binder. Powder form of the sample was used for structural study while pellets were utilized for wettability experiments.

## RESULTS AND DISCUSSION:

## PHASE IDENTIFICATION:

With the help of Debye Scherrer's equation the average crystalline size of LaAlO<sub>3</sub> perovskite powder was determined.

$$t = \frac{0.9\lambda}{\beta \cos\theta}$$

Where,  $t$  is the average size of the particles,  $\lambda$  is wavelength of X-ray radiation;  $\beta$  is the full width at half maxima of the diffracted peak and  $\theta$  is the angle of diffraction.

Nanocrystals of LaAlO<sub>3</sub> are more attractive in the field of catalytic application. Figure 1 shows the XRD pattern of mixed precursor calcined in air at 800°C for 4 hours. It clearly shows that crystalline phase formation takes place above 750°C. This diffraction pattern corresponds to the peaks of (0 1 2), (1 1 0), (2 0 2), (0 2 4), (1 1 6), (3 0 0), (2 2 0) and (3 1 2). These polycrystalline nanoparticles exhibited rhombohedral structure of LaAlO<sub>3</sub> (JCPDS No. 31-0022). The calculated lattice parameter  $a = 5.364 \text{ \AA}$  was in good agreement with the reported value [9]. An average crystalline size of the system is calculated by Debye Scherrer's equation to the half intensity width of (1 1 0) peak. From this equation, average size of LaAlO<sub>3</sub> nanoparticles was estimated to be 14 nm.

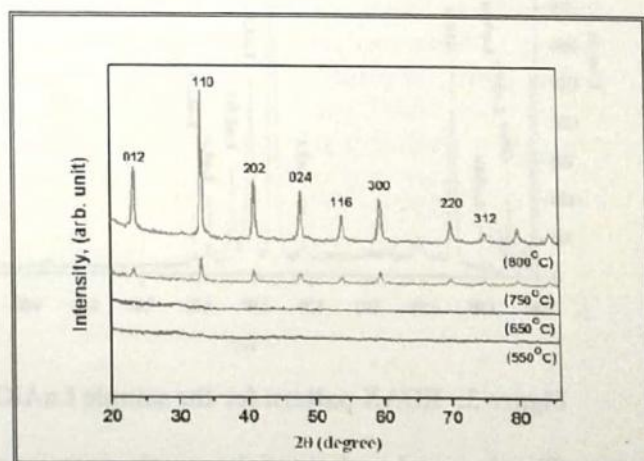


Figure 1: XRD pattern of LaAlO<sub>3</sub>

## SCANNING ELECTRON MICROSCOPY (SEM):

Surface morphology of the samples was studied using scanning electron microscope (SEM) [JEOL, JED-2300].

The SEM image of pure  $\text{LaAlO}_3$  showed that the  $\text{LaAlO}_3$  particles are non-uniform in size along with agglomeration owing to particle-particle interactions (Figure 2). Also, the images revealed that the product has low density, loose and porous nature. Thus, the material is found suitable for gas sensing applications [10,11]. The powder was found to have a spongy aspect and consisted of agglomerates as well as large number of pores. The pore size of  $\text{LaAlO}_3$  particles was in the range of 0-2  $\mu\text{m}$ .

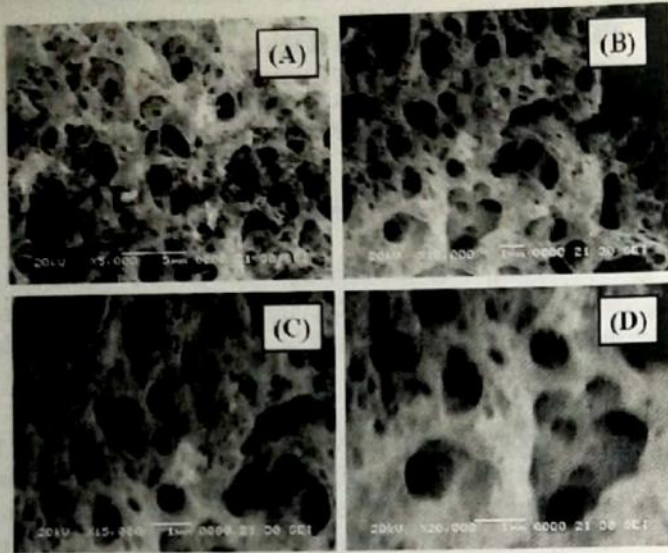


Figure 2: SEM images of  $\text{LaAlO}_3$  composite

From a typical surface micrograph (Figure 2), it indicates that the composite is highly porous and nanocrystalline in nature.

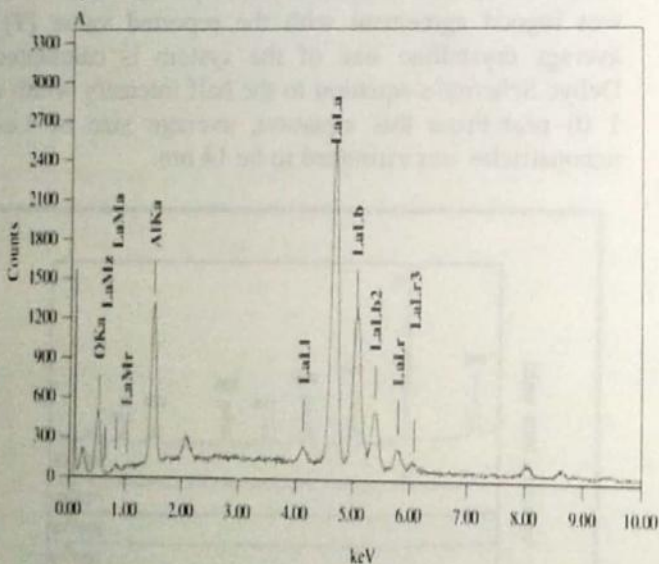


Figure 3: EDAX pattern for the sample  $\text{LaAlO}_3$

The elemental analysis of the sample was carried out by using energy dispersive X-ray spectrometer (EDS) and is shown in Figure 4. The stoichiometric mass percentage of La, Al and O in  $\text{LaAlO}_3$  is 64.94, 12.62 and 22.44 respectively. However, we found the mass percent La, Al and O in  $\text{LaAlO}_3$  synthesized material as 82.57, 10.71 and 6.72. The synthesized material is thus oxygen deficient and

excess in La and Al elements, indicating n-type nature of the material.

This was carried out to understand the composition of Lanthanum, Aluminium and Oxygen in the material. The EDS result clearly shows that  $\text{LaAlO}_3$  contains La, Al, and O without any impurity. Quantitative EDX analysis verified that doping with lanthanum is close to the expected concentration.

### TRANSMISSION ELECTRONMICROSCOPY(TEM):

The TEM specimens were prepared by placing microdrops of colloidal samplesolutions on a carbon film supported by a copper grid. The TEM images of the nanocrystalline  $\text{LaAlO}_3$  calcinated at  $850^\circ\text{C}$  in air for 4 hours were depicted as in Figure 4. It indicated the presence of  $\text{LaAlO}_3$  nanoparticles with 35-45 nm size which illustrated spherical morphology of oriental aggregation, agglomeration and polymeric linkage throughout the region. Well developed, spherical pores with 40-70 nm size were formed.

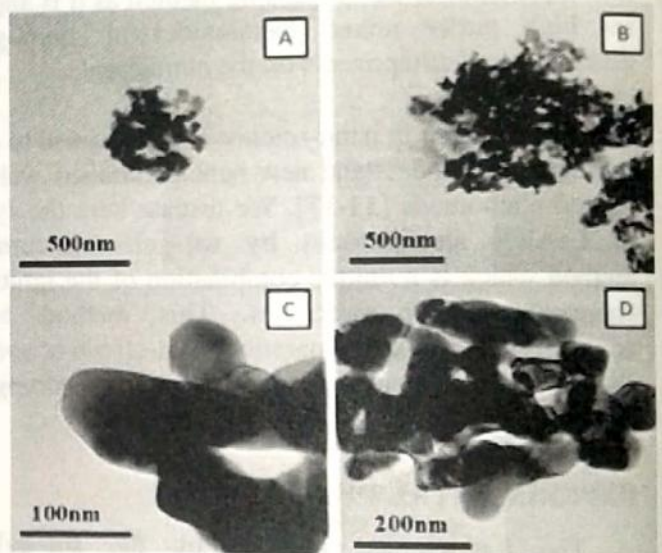


Figure 4: TEM micrographs of the powder calcinated at  $850^\circ\text{C}$

At higher resolution, the SEM and TEM images demonstrated that the particles are most irregular in shape within a nanosize range.

### WETTABILITY EXPERIMENT:

Thomas Young had described the force acting on a liquid droplet spreading on surface termed as contact angle ( $\theta$ ) is related to the interfacial energies acting between the solid-liquid ( $\gamma_{SL}$ ), solid-vapor ( $\gamma_{SV}$ ) and liquid-vapor ( $\gamma_{LV}$ ) given by relation.

$$\cos \theta = \frac{(\gamma_{SV} - \gamma_{SL})}{\gamma_{LV}} \quad (1)$$

The expression given by Equation 2 is strictly valid only for surfaces that are atomically smooth, chemically homogeneous and those that do not change their characteristics due to interactions of the probing liquid with the substratum or any other outside force.

$$\cos \theta^* = r \cos \theta \dots\dots\dots$$

(2)

Where  $r$  is the roughness factor of surface

Considering above equation we evaluated contact angle of Lanthanum Aluminium oxide and it was found to be exactly zero degree. Theoretical contact angle value of super hydrophilic material is found to be in between zero to five degree. Result shows that our material is super hydrophilic in nature, the highly rough surface nature clearly seen from the following images (Figure 5) with consideration given to the surface roughness.

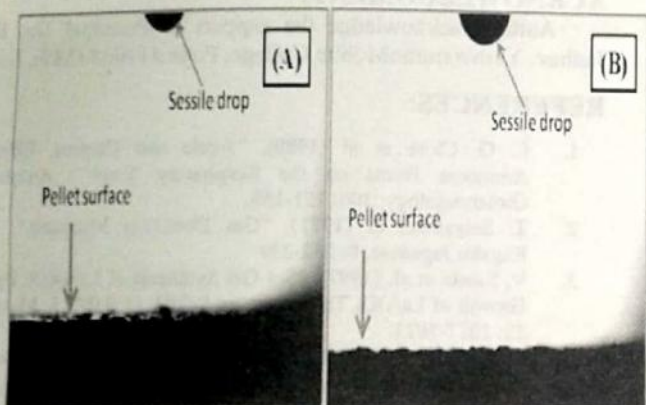


Figure 5: Photograph of measured contact angle on rough surface of LaAlO<sub>3</sub> material

**SENSING PERFORMANCE OF THE SENSOR:**

**Measurement of gas response, selectivity, response and recovery time**

The ratio of the change in conductance of the sensor on exposure in the target gas to the original conductance in air is the Gas Response (S).

The relation for S is as:

$$S = \frac{G_g - G_a}{G_a}$$

Where,  $G_a$  and  $G_g$  are the conductance of sensor in air and in target gas medium, respectively.

**Sensing performance of pure LaAlO<sub>3</sub> pellet:**

**a) Effect of operating temperatures:**

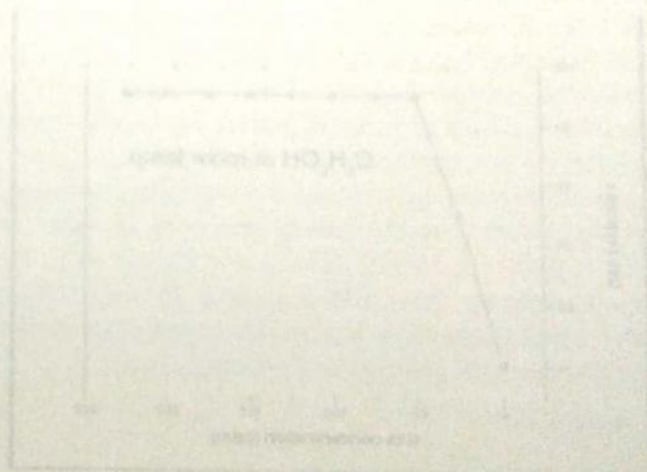
The gas response of LaAlO<sub>3</sub> pellet was determined over a range of operating temperatures from room temperature to 400 °C. The results are shown in Table 1.

The response for LPG (100 ppm) was directly proportional to the temperature i.e. it increased with increase in temperature. Maximum response was observed at 400 °C. The response for NH<sub>3</sub> increased up to 250 °C and decreased with further increase in temperature. The ethanol response at room temperature is expected to be monitored by adsorption of moisture on the LaAlO<sub>3</sub> pellet.

Operating temperature (°C)	Gas response for various gases						
	LPG	CO <sub>2</sub>	NH <sub>3</sub>	C <sub>2</sub> H <sub>5</sub> OH	H <sub>2</sub>	Cl <sub>2</sub>	H <sub>2</sub> S
30	0.01	0.04	0.31	2.93	0.01	0.01	0.12
100	0.04	0.05	0.57	1.48	0.02	0.03	0.33
150	0.11	0.07	0.99	1.39	0.04	0.04	0.48
200	0.21	0.09	1.58	1.31	0.06	0.09	0.53
250	0.22	0.12	1.98	0.94	0.08	0.11	0.64
300	0.34	0.21	1.69	0.54	0.09	0.12	0.87
350	0.79	0.96	1.52	0.68	0.11	0.39	0.69
400	1.08	0.32	1.03	1.09	0.1	0.72	0.45

Table 1: Gas responses of LaAlO<sub>3</sub> pellet over a range of operating temperatures

Figure 6 shows the variation of responses of LaAlO<sub>3</sub> for various gases. Need to discuss the graphs.....also the formulae in the diagrams are not in mentioned appropriately.



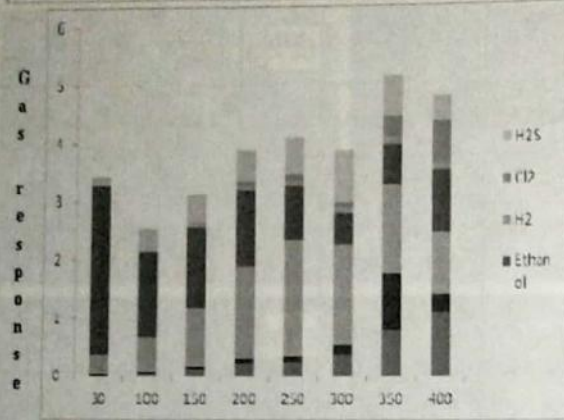
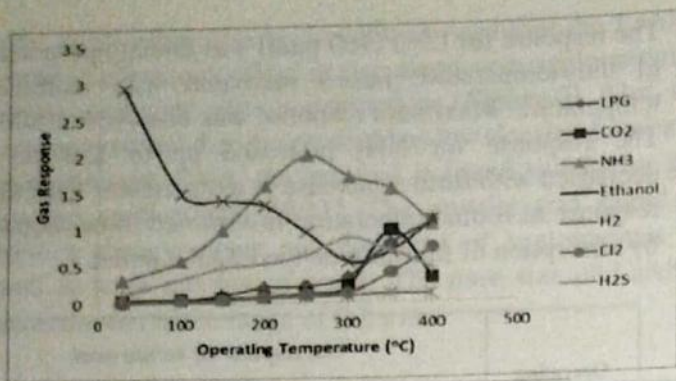


Figure 6 Variation of different gas responses with operating temperature

b) Effect of ethanol gas at room temperature (Active Region)

Figure 7 represents variation of gas response of the  $\text{LaAlO}_3$  sample with ethanol ( $\text{C}_2\text{H}_5\text{OH}$ ) gas concentration at room temperature. When pellet was exposed to varying concentrations of ethanol response values increased with increasing gas concentration upto 50 ppm at room temperature. The rate of increase in responses was relatively larger up to 60 ppm. This denotes that the active region of the sensors would be at 60 ppm gas concentration. Gas molecules will be formed on the sensor surface, at lower concentrations, which interacts actively giving larger response [18-23]. Beyond 60ppm, gas concentration would result in saturated response due to formation of multilayer gas molecules on sensor surface.

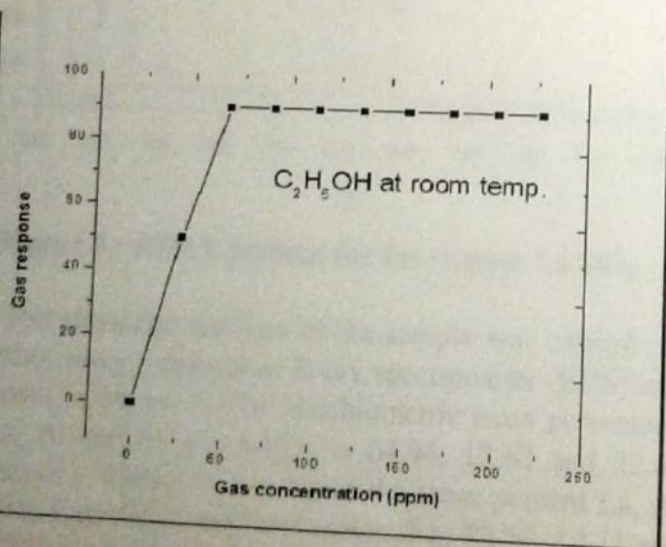


Figure7: Variation of different gas responses with operating temperature

CONCLUSION:

Nanocrystalline  $\text{LaAlO}_3$  particles prepared by sol-gel auto-combustion method are highly porous with average particle size 30 to 40nm. Phase formation of the  $\text{LaAlO}_3$  was investigated by XRD techniques. The synthesized product showed single phase of rhombohedral structure. The grain size calculated by Debye Scherrer's equation was found to be 14 nm. Surface morphology was studied by scanning electron microscopy (SEM) and transmission electron microscopy (TEM). Highly porous and nanocrystalline compounds were obtained which were found to be useful for gas sensitivity and selectivity.  $\text{LaAlO}_3$  demonstrated noteworthy activity in promoting the ethanol gas sensing and showed highest response at room temperature. The sensor has good selectivity to ethanol against ammonia and LPG at room temperature.

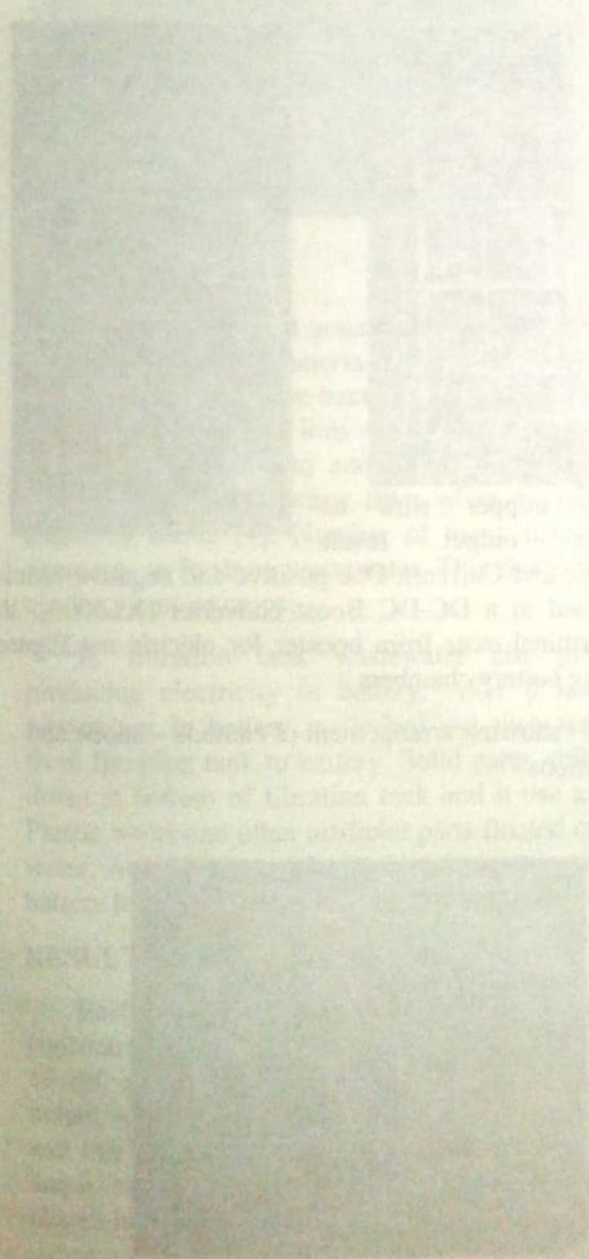
ACKNOWLEDGMENT:

Authors acknowledge the support of Principal Dr. K. D. Jadhav, Yashwantrao Mohite College, Pune 411038 (MS), India.

REFERENCES:

1. L. G. Close et al (1980), "Acute and Chronic Effects of Ammonia Burns on the Respiratory Track", Archives of Otolaryngology, 106: 151-158.
2. T. Seiyama et al (1971), "Gas Detecting Materials", Zairyo Kagaku Japanese, 8: 232-239.
3. V. Sandu et al. (1997), "Sol-Gel Synthesis of  $\text{LaAlO}_3$ : Epitaxial Growth of  $\text{LaAlO}_3$  Thin Films on  $\text{SrTiO}_3$  (1 0 0)", J. Mater. Res. 12: 1017-1021.
4. M. D. Kumaret al (1995), "Synthesis of lanthanum aluminate by citrate-combustion route", Materials Letters, 25: 171-174.
5. S. Ranet al (2008), "Synthesis of  $\text{LaAlO}_3$  powder using triethanolamine", Ceramics International, 34: 443-446.
6. WenJihua et al (2006), "Preparation of spinel-type  $\text{Cd}_{1-x}\text{Mg}_x\text{Ga}_2\text{O}_4$  gas-sensing material by sol-gel method" Sensors and Actuators B: Chemical, 115: 622-625.
7. J. Chandradaset al (2010), "Mixture of fuels approach for the solution combustion synthesis of  $\text{LaAlO}_3$  Nanopowders" Advanced Powder Technology 21: 100-105.
8. M. Chroma et al (2005), "Processing and characterization of sol-gel fabricated mixed metal aluminates", Ceramics International 31: 1123-1130.
9. A. Barrera et al (2007), "Structural properties of  $\text{Al}_2\text{O}_3$ - $\text{La}_2\text{O}_3$  binary oxides prepared by sol-gel", Materials Research Bulletin 42: 640-648.
10. H. M. O'Bryan, et al. (1990), "Thermal analysis of rare earth gallates and aluminates", Journal of Materials 5: 183-189.
11. D. R. Patil et al (2006), "Preparation and Study of  $\text{NH}_3$  Gas Sensing behavior of  $\text{Fe}_2\text{O}_3$  Doped  $\text{ZnO}$  Thick Film Resistors" Sensors and Transducers 70: 661-670.
12. K. A. Khamkaret al (2013), "Synthesis, characterization and electrical properties of nanostructured  $\text{LaAlO}_3$  by sol-gel auto-combustion method", J Mater Sci: Mater. Electron, 10854:1428-33.
13. K. Vidyasagaret al (1985), "Synthesis of complex metal oxides using hydroxide, cyanide, and nitrate solid solution precursors" Solid State Chem. 58: 29-37.
14. A. M. G. Pedrosa et al (2005), "Synthesis and Catalytic Properties of Lanthanum Nickelate Perovskite Materials", Reaction Kinetics and Catalysis Letters, 84: 3-9.

15. D. Zhou et al (2004), "Synthesis of  $\text{LaAlO}_3$  via Ethylene diamine tetra acetic Acid Precursor", *Materials Chemistry and Physics*, 84: 33-36.
16. P. Peshevetal(1994), "Preparation of lanthanum aluminate thin films by a sol-gel procedure using alkoxide precursors", *Mater. Res. Bull.*, 29: 255-261.
17. V. S. Krylovetal(1973), "Preparation of rare earth aluminates from aqueous solutions", *NeorganicheskieMaterialy*, 9: 1388-1390, (Russian).
18. N. S. Ramgiret al (2013), "Ethanol sensing properties of pure and Au modified ZnO nanowires", *Sensors and Actuators B: Chemical*, 187: 313-318.
19. A. S. Zoolfakaret al (2013), "Nanostructured copper oxides as ethanol vapour sensors", *Sensors and Actuators B: Chemical*, 185: 620-627.
20. G. Qinet al (2013), "Synthesis of Sr and Mg double-doped  $\text{LaAlO}_3$ nanopowders via EDTA-glycine combined process", *Powder Technology*, 235: 880-885.
21. M. S. Waghet al (2006), "Modified zinc oxide thick film resistors as  $\text{NH}_3$  gas sensor", *Sens. Actuat. B: Chem.*, 115:128-133.
22. B. Karunagaranetal(2007), " $\text{TiO}_2$  thin film gas sensor for monitoring ammonia", *Mater. Charact.* 58: 680 - 684.
23. X. Wang et al(2000), "Study of  $\text{WO}_3$  - based sensing materials for  $\text{NH}_3$  and  $\text{NO}$  detection", *Sens.Actuat. B-Chem.* 66:74-76.



1

2

3

4

5

6

7

8

9

10

11

12

13

14

15

16

17

18

19

20

21

22

23

24

25

26

27

28

29

30

31

32

33

34

35

36

37

38

39

40

41

42

43

44

45

46

47

48

49

50

51

52

53

54

55

56

57

58

59

60

61

62

63

64

65

66

67

68

69

70

71

72

73

74

75

76

77

78

79

80

81

82

83

84

85

86

87

88

89

90

91

92

93

94

95

96

97

98

99

100